Received July 2001
Accepted April 2002

Investigation into a confined laminar swirling jet and entropy production

S.Z. Shuja, B.S. Yilbas and M.O. Budair
King Fahd University of Petroleum and Minerals, Dhahran, Saudi Arabia

Keywords *Jets, Flow, Temperature*

Abstract *A confined laminar swirling jet is an interesting research topic due to flow and temperature fields generated in and across the jet. In the present study, a confined laminar swirling jet is studied, and flow and temperature fields are simulated numerically using a control volume approach. In order to investigate the influence of the jet exiting (exiting the nozzle and inleting to the control volume) velocity profiles on the flow and heat transfer characteristics, eight different velocity profiles are considered. To identify each velocity profile, a velocity profile number is introduced. Entropy analysis is carried out to determine the total entropy generation due to heat transfer and fluid friction. Merit number is computed for various swirling velocities and velocity profiles. It is found that swirling motion expands the jet in the radial direction and reduces the jet length in the axial direction. This, in turn, reduces the entropy generation rate and improves the Merit number. Increasing velocity profile number enhances the entropy production rate, but improves the Merit number.*

Nomenclature

A = Nozzle exit area
h = Enthalpy
$\dot{I}$ = Irreversibility rate
k = Thermal conductivity
M = Merit number
$\dot{m}$ = Mass flow rate
n = Velocity profile number
p = Pressure
$\dot{Q}$ = Heat transfer rate
r = Distance in the radial direction
r_o = Radius of the nozzle exit
Re = Reynolds number
S_ϕ = Deriving term for variable ϕ
S'''_{gen} = Volumetric entropy generation rate
$\dot{S}_{gen}$ = Integrated entropy generation rate
T = Temperature
T_{amb} = Ambient or reference temperature
T_{jet} = Jet temperature
$\forall$ = Volume
U = Swirl velocity
V = Velocity in the radial direction
W = Velocity in the axial direction
$\bar{W}$ = Mean velocity in the axial direction

Greek

Γ_ϕ = Exchange coefficient for ϕ
μ = Dynamic viscosity
ρ = Density
σ = Prandtl number
Φ = Viscous dissipation
ϕ = Arbitrary variable

Subscript

amb = Ambient
in = Conditions at inlet
jet = Conditions at jet
max = Maximum

The authors acknowledge the support of King Fahd University of Petroleum and Minerals, Dhahran, Saudi Arabia, for this work.

International Journal of Numerical Methods for Heat & Fluid Flow, Vol. 12 No. 7, 2002, pp. 870-887.

DOI 10.1108/09615530210443070

1. Introduction

Confined jets find wide applications in industry, such as thermal spraying, combustion systems, etc. The swirling is introduced in confined jet flow to generate a tangential velocity gradient, which in turn results in central recirculation zone, in which case the shear layer between the reverse flow and surrounding forward flow stabilizes the flow field in the confined system. Moreover, the heat transfer characteristics of the jet flow alters considerably once the swirling motion at jet inlet is introduced. The entropy generation in the system enables to identify the frictional losses and heat transfer rates in the system. Consequently, investigation into flow and heat transfer characteristics as well as entropy generation in confined swirling jet flow is essential.

Considerable research studies were carried out to explore the swirling flow characteristics. The recirculation zones of unconfined and confined annular swirling jets were examined by Sheen *et al.* (1996). They introduced scaling analysis to correlate the lengths of the recirculation zone with the swirl numbers. They showed that the recirculation length was inversely proportional to the ratio of azimuthal velocity to the axial velocity. The characteristics of swirling flow in a circular pipe were investigated experimentally by Li and Tomita (1994). They developed empirical correlations for the static and dynamic pressure variations due to swirling motion of the fluid. A numerical study of a confined strong swirling flow was carried out by Nikjooy and Mongia (1991). They indicated that the inlet kinetic energy dissipation was highly affected by the stress field and the mean velocity was influenced by the size of the recirculation zone. The stability of a compressible axisymmetric swirling jet was studied by Khorrami (1995). He showed that the stabilizing influence of increasing Mach number was diminished with the introduction of swirl to the jet flow. The heat transfer characteristics in laminar wall jets with different initial velocity profiles were investigated by Korovkin and Sokovishin (1989). They developed the correlation between the temperature field and initial velocity profiles.

Entropy analysis provides useful information on the irreversibility associated with a system. The irreversibility in the flow system is generated due to fluid friction and heat transfer. Moreover, the frictional loss results in pressure drop while the heat transfer causes temperature change in the system. Consequently, the entropy analysis gives insight into the amount of irreversibility that is associated with the frictional loss and heat transfer rates. This provides useful information for the thermal system operation and design (Drost and White, 1991). In a thermo-fluid system, entropy is generated due to fluid friction and heat transfer. Moreover, when the heat transfer rate is high, the entropy generation due to heat transfer, in general, dominates over the entropy generation because of fluid friction. Considerable research studies were carried out to explore the entropy generation in thermal systems. Numerical predictions of local entropy generation in an impinging jet was studied by

Drost and White (1991). They indicated that the calculation of local entropy generation was feasible and could provide useful information. Entropy generation due to isothermal cylinder in cross flow was investigated by Abu-Hijleh (1998). He showed that large diameter cylinders resulted in low entropy generation. Entropy generation in conjugate heat transfer from a discretely heated plate to an impinging confined jet was studied by Ruocco (1997). He indicated that entropy generation allowed us to assess preliminary the conjugate arrangement based on solid-fluid coupling criteria. The entropy production rate for a sensible thermal storage system was investigated by Maveety and Razani (1996). They showed that the optimal flow rate depended on the terminal removal time, which was related to the entropy production rate.

In the present study, a confined laminar swirling jet with different jet velocity inlet profiles is considered. In order to account for the heat transfer taking place between the jet and its surroundings, the jet temperature is taken higher than its ambient temperature. A numerical scheme using a control volume approach is introduced when discretizing the governing equations of flow and energy. The study is extended to include four swirling velocities and seven velocity profile numbers.

2. The mathematical model

2.1 Flow and energy equations

The set of partial differential equations governing a steady flow field with constant swirl for an axisymmetric flow situation can be written in cylindrical polar coordinates as:

$$\frac{\partial}{\partial z}\left(\rho U\phi - \Gamma_\phi \frac{\partial \phi}{\partial z}\right) + \frac{1}{r}\frac{\partial}{\partial r}\left(\rho r V\phi - \Gamma_\phi r \frac{\partial \phi}{\partial r}\right) = S_\phi \tag{1}$$

In equation (1), ϕ is a general variable, Γ_ϕ is the exchange coefficient for the property ϕ, S_ϕ is the deriving expression for ϕ. In the most general form, it may comprise a term for the rate of generation of ϕ per unit volume together with other terms that cannot be included on the left hand side of equation (1).

Equation (1) becomes the conservation for mass, axial momentum, radial momentum, tangential momentum and energy equations when setting $\phi = 1$, W, V, U and T, respectively. Equation (1) is the compactly represented elliptic partial differential equation, and the list of the dependent variables and the associated definitions of Γ_ϕ and S_ϕ are given in Table I.

2.2 Boundary conditions

The boundaries of the solution domain and symmetry axis are shown in Figure 1. The relevant boundary conditions are given as:

Inlet to control volume: ($z = 0$; and $0 \le r \le r_o$)

$$U_{in} = \text{specified}, \quad \bar{W}_{in} = \text{specified } (0.03\,\text{m/s}) \quad \text{and} \quad T_{in} = \text{specified } (310\,\text{K}) \tag{2}$$

where r_o is the nozzle exit diameter ($r_o = 0.0127$ m). Since the mass flow rate is kept constant during the simulations, the mean jet velocity in the axial direction at inlet to the control volume ($\bar{W}_{in}$) is kept constant. The velocity profile exiting the nozzle and entering the control volume is considered as:

$$W_{in} = W_{max}\left[1 - \left(\frac{r}{r_o}\right)\right]^n$$

where r_o is the nozzle exit diameter and W_{max} is the maximum axial velocity component at the nozzle exit. The mean velocity of the flow at nozzle exit can be determined from the constant volume flow rate as:

$$\bar{W}_{in} = \frac{1}{A}\int_0^{r_o} 2\pi r W_{max}\left[1 - \left(\frac{r}{r_o}\right)\right]^n \mathrm{d}r$$

where n is the velocity profile number and its values are given in Table II, and A is the nozzle exit area (πr_o^2).

Outlet to control volume: (at $z = 0$, $r_o < r \le 0.05$ and at $z = 0.30$, $0 \le r \le 0.05$)

It is considered that the flow extends over a sufficiently long domain, therefore, it is fully developed at the outlet sections. Thus, for a variable ϕ the condition is

$$\frac{\partial(r\phi)}{\partial x} = 0 \tag{3}$$

where x is the arbitrary outlet direction. The mass flow rate remains constant at the outlet section.

Conservation of	ϕ	Γ_ϕ	S_ϕ
Mass	1	0	0
Axial momentum	W	μ	$-\frac{\partial p}{\partial z} + \frac{\partial}{\partial z}\left(\mu\frac{\partial U}{\partial z}\right) + \frac{1}{r}\frac{\partial}{\partial r}\left(r\mu\frac{\partial V}{\partial z}\right)$
Radial momentum	V	μ	$-\frac{\partial p}{\partial r} + \frac{\partial}{\partial z}\left(\mu\frac{\partial W}{\partial z}\right) + \frac{1}{r}\frac{\partial}{\partial r}\left(r\mu\frac{\partial V}{\partial r}\right) - 2\mu\frac{V}{r^2} + \rho\frac{U^2}{r}$
Tangential momentum	U	μ	$-\left(\frac{\mu}{r^2} + \rho\frac{V}{r} + \frac{1}{r}\frac{\partial\mu}{\partial r}\right)U$
Temperature	T	μ/σ	$\mu\Phi$

Table I. Variables and the corresponding conservation equations

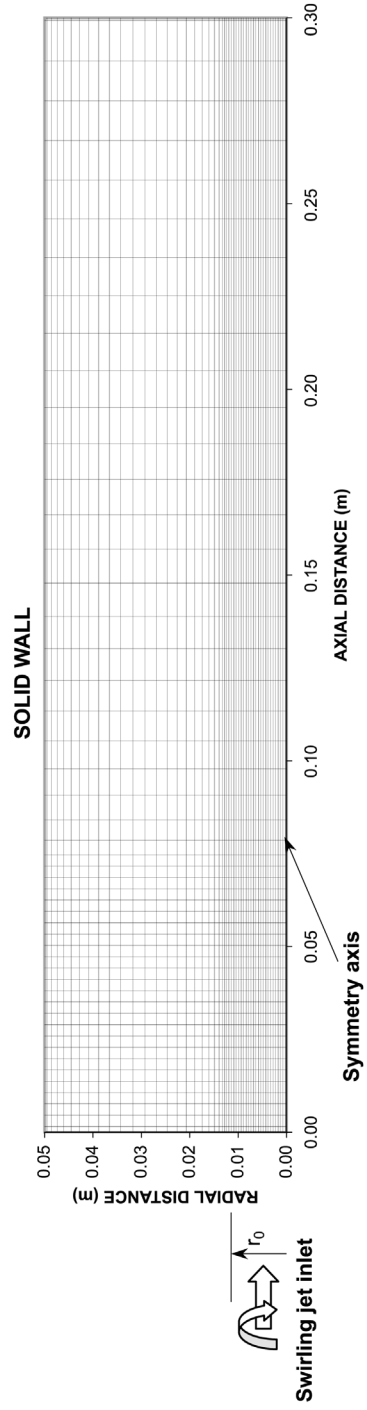

Figure 1.
Schematic view of the solution domain and grid used for the computations ($r_o = 0.0127$ m)

Symmetry axis: ($r = 0$)

The radial derivative of the variables is set to zero at the symmetry axis, i.e.:

$$\frac{\partial \phi}{\partial r} = 0 \quad \text{and} \quad V = 0 \tag{4}$$

Solid wall–fluid interface: ($z = 0$ and $z = 0.3$, $r = 0.05$)

The adiabatic solid wall is assumed, i.e.:

$$k_{\text{gas}} \frac{\partial T_{\text{w}_{\text{gas}}}}{\partial z} = 0$$

No slip condition is considered at the solid wall, i.e.

$$W = V = U = 0$$

2.3 Entropy, irreversibility and heat transfer analysis

The non-equilibrium process of exchange and momentum transfer within the fluid and at the solid boundaries results in continuous entropy generation in the flow system. The local entropy generation rate per unit volume for an incompressible Newtonian fluid may be written as (Bejan, 1982):

$$S'''_{\text{gen}} = \frac{k}{T^2}(\nabla T)^2 + \frac{\mu}{T}\Phi \tag{5}$$

or

$$(S'''_{\text{gen}})_{\text{cond}} = \frac{k}{T^2}(\nabla T)^2 \quad \text{and} \quad (S'''_{\text{gen}})_{\text{fric}} = \frac{\mu}{T}\Phi$$

where in polar coordinates;

$$\Phi = 2\left[\left(\frac{\partial V}{\partial r}\right)^2 + \left(\frac{V}{r}\right)^2 + \left(\frac{\partial W}{\partial z}\right)^2\right] + \left(\frac{\partial U}{\partial z}\right)^2 + \left(\frac{\partial V}{\partial z} + \frac{\partial W}{\partial r}\right)^2 + \left(\frac{\partial U}{\partial r} - \frac{U}{r}\right)^2$$

Here $(S'''_{\text{gen}})_{\text{cond}}$ represents the entropy generation per unit volume due to heat transfer and $(S'''_{\text{gen}})_{\text{fric}}$ is the entropy generation per unit volume due to fluid friction.

The total entropy generation rate over the volume can be written as:

$$\dot{S}_{\text{gen}} = \oint_{\forall} S'''_{\text{gen}}\, \mathrm{d}\theta\, \mathrm{d}z\, r\, \mathrm{d}r$$

Table II. Velocity profile numbers and swirl velocities used in the simulation

n	1	1/1.5	1/2	1/5	1/7	1/10	1/200
U (m/s)	0.01	0.02	0.03	0.04			

where ∀ is the volume. The rate of total irreversibility is defined as:

$$\dot{I} = T_{\text{amb}}\dot{S}_{\text{gen}}$$

The heat transfer rate to the fluid can be written as:

$$\dot{Q} = \dot{m}_{\text{in}}C_p(T_{\text{jet}} - T_{\text{amb}} = \dot{m}_{\text{jet}}C_p[T_{\text{jet}} - T_{\text{amb}}]$$

where

$$\dot{m}_{\text{jet}} = \int_0^{r_o} \rho_i W_i 2\pi r \, \mathrm{d}r.$$

The rate of energy transfer accompanying energy transfer at the rate of $\dot{Q}$ is given as (Mukherjee *et al.*, 1987):

$$\dot{Q}_a = \dot{Q}\left(1 - \frac{T_{\text{amb}}}{T_{\text{jet}}}\right)$$

where T_{amb} is the ambient or reference temperature, which is considered energy reference environment temperature and T_{jet} is the jet temperature at nozzle exit.

The Merit number is defined as the ratio of energy transferred to the sum of energy transferred and energy destroyed (Mukherjee *et al.*, 1987), i.e.:

$$M = \frac{\dot{Q}_a}{\dot{Q}_a + \dot{I}}$$

or:

$$M = \frac{\dot{Q}\left(1 - \frac{T_{\text{a}}}{T_{\text{w}}}\right)}{\dot{Q}\left(1 - \frac{T_{\text{a}}}{T_{\text{w}}}\right) + \dot{I}} \tag{6}$$

3. Numerical solution of governing equations

The control volume approach is used in the numerical scheme to discretize the governing equations. The mathematical details of the discretization process can be found in the world reported by Patankar (1980). For the purpose of solution the flow domain is overlaid with a rectangular grid as shown in Figure 1 whose intersection points (nodes) denote the location at which all variables, with the exception of the velocities, are calculated. The latter are computed at locations midway between the pressure which drive them. The staggered grid arrangement provides handling the pressure linkages through the continuity

equation and is known as the SIMPLE algorithm (Patankar, 1980). This method is an iterative process to the steady-state convergence. The pressure link between the continuity and the momentum is accomplished by transforming the continuity equation into a Poisson equation for pressure. The Poisson equation implements a pressure correction for a divergent velocity field. The steady-state convergence is achieved by successively predicting and correcting the velocity components and the pressure. An initial guess for the pressure variable at each grid point is introduced.

The grid independent tests are carried out to ensure the grid independent results, consequently, the grid size and the grid orientation giving the grid independent results are selected. The mesh used in the present study have 2,500 (50×50) nodal points as shown in Figure 1.

4. Results and discussions

A confined laminar swirling jet with different swirling velocities and jet inlet velocity profiles is simulated. The flow and temperature fields are predicted using a numerical scheme employing a control volume approach. Entropy production in the flow system is analyzed and the entropy production rate predicted. The simulation conditions and fluid properties are given in Table I. Although the axial distance (z) extends to 0.3 m, figures are plotted to a maximum axial length of 0.2 m. This is because of the flow structure, which does not change along the distance $z = 0.2$ m to $z = 0.3$ m.

Figure 2 shows the velocity vectors for three jet inlet velocity profiles with and without swirling. The jet inlet profiles are described by the jet velocity profile number in the text. The influence of jet profile number on the flow field is considerable. In this case, triangle-like profile ($n = 1$) results in rather smooth velocity field around the jet as compared to uniform-like jet velocity profile ($n = 1/200$), i.e. uniform-like jet velocity profile results in circulation cell in the region next to jet exiting. The size of circulation cell increases with swirling velocity. The shear layer between the jet and its surrounding flow results in momentum transfer, which in turn enhances the size of the circulation cell in this region. The influence of the swirling on the downstream flow diminishes beyond the distance five times of the jet radius in the axial direction. This can be observed when comparing the velocity vectors corresponding to swirling and non-swirling situations. The size of the jet enlarges (expands) as the jet exiting velocity becomes uniform-like ($n = 0.005$). This is more pronounced for the swirling situations. In this case, the circulation cell next to the jet exiting becomes visible. Since the mass flow rate in the jet remains constant, a uniform-like velocity profile results in the velocity profile with low magnitude at the nozzle exit. Consequently, lowering the jet velocity magnitude and increasing the swirl velocity at the nozzle exit result in expansion of the jet. Moreover, expanding jet and its surrounding flow result in shear layer in the region close to the jet boundary. This, in turn, generates a circulation cell next

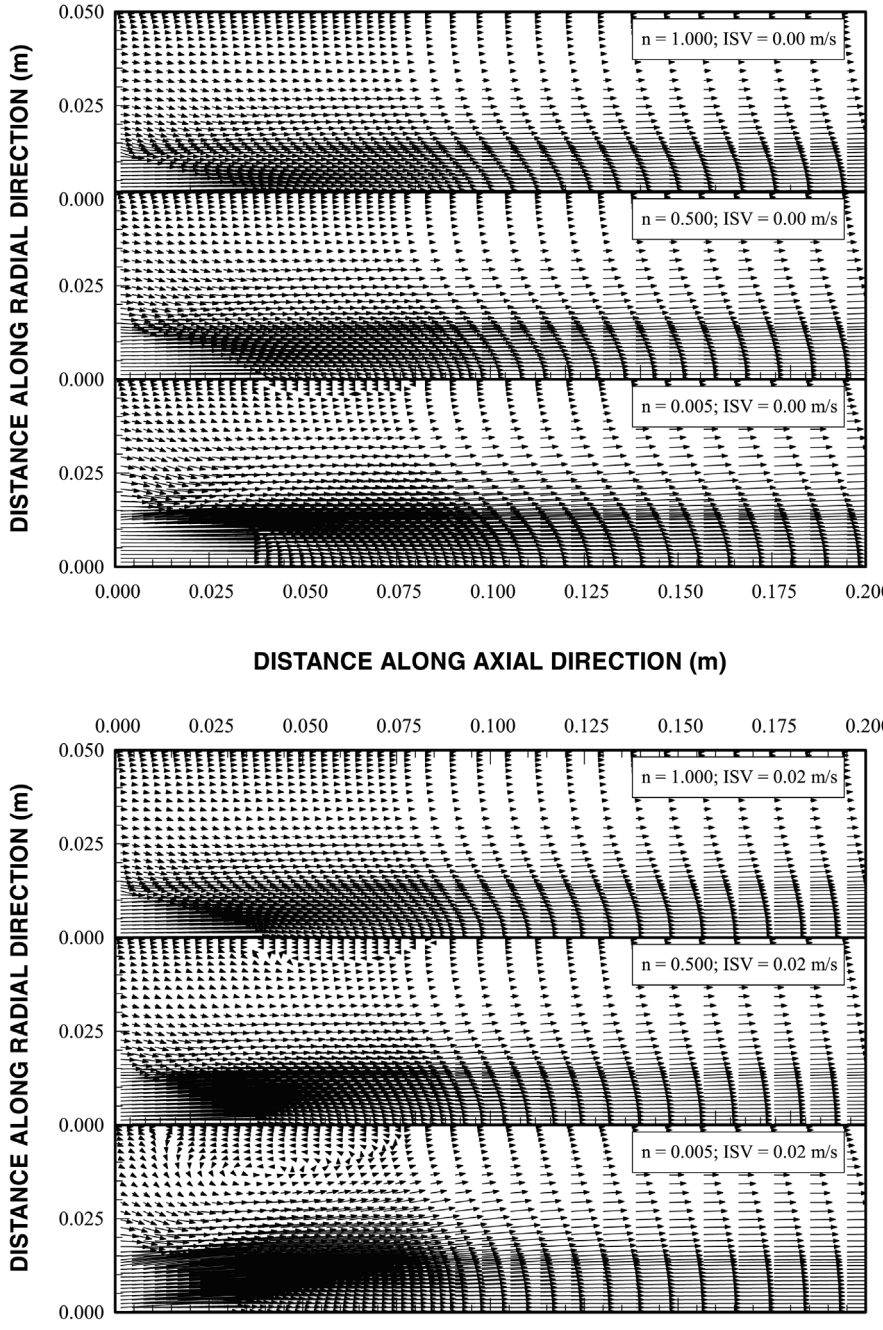

Figure 2.
Velocity vectors corresponding to different flow configurations. *n* is a velocity profile number and ISV represents the inlet swirl velocity

to the jet boundary. The expansion of the jet is also evident from radial velocity distributions, which are shown in Figure 3a. The circulation cell in the region next to the jet boundary has no component in the radial direction. This indicates that the circulation occurs in the axial direction (Figure 3b) and the radial velocity component of the circulation cell is zero.

Figure 4 shows the temperature contours for different jet exiting velocity profiles and swirling situations. Temperature contours follow almost axial velocity profiles in the jet. This is because of the laminar jet where flow mixing in the jet is minimal. Moreover, temperature profiles in the circulation cell do not follow the velocity profiles, since the circulation cell is formed next to the jet boundary in the surrounding fluid. It should be noted that the jet temperature exiting the nozzle and inleting the control volume is kept as 310 K while the fluid sucked in, due to low-pressure attainment next to the jet boundary, from the free boundary next to the jet exit is at 300 K. The parabolic-like jet velocity profile ($n = 0.5$) results in extension of jet in the axial direction. In this case, the hot jet stream extends further into the downstream. In the case of swirling, the extension of gas jet in the axial direction reduces, which is more pronounced for the uniform-like velocity profile.

Figure 5 shows the total entropy contours along the axial direction for three different velocity profiles and swirling situations. It should be noted that the entropy generation due to fluid friction is considerably smaller than its counterpart corresponding to the heat transfer; therefore, the total entropy generation is presented in the figure. Entropy contours are very dense in the region close to the jet exit and they do not extend in the axial and radial directions considerably. The triangle-like velocity profile results in larger extension of the entropy contours in the axial direction than those corresponding to other jet exiting velocity profiles. This is because of the extension of temperature contours in the axial direction. It should be noted that the entropy generation due to heat transfer dominates over the entropy generation due to fluid friction, i.e. the ratio is almost 10. Consequently, the flow field resulting in high temperature gradient produces more entropy than those with small temperature gradients. This can be observed from uniform-like velocity profile, i.e. small extension of temperature profiles in the axial direction occurs. Swirling velocity reduces the entropy generation. In this case, increasing swirling enhances the jet expansion which in turn reduces the temperature gradient across the jet boundary. This is more pronounced for uniform-like jet velocity profile.

Figure 6 shows the normalized total entropy generation with velocity profile number for different swirl velocities. The total entropy generation increases with increasing velocity profile number. In this case, triangle-like velocity profile ($n = 1$) results in high temperature gradient across the jet and its surrounding as well as heated fluid in the jet extends considerably in the axial direction. Consequently, large temperature gradient across the jet boundary

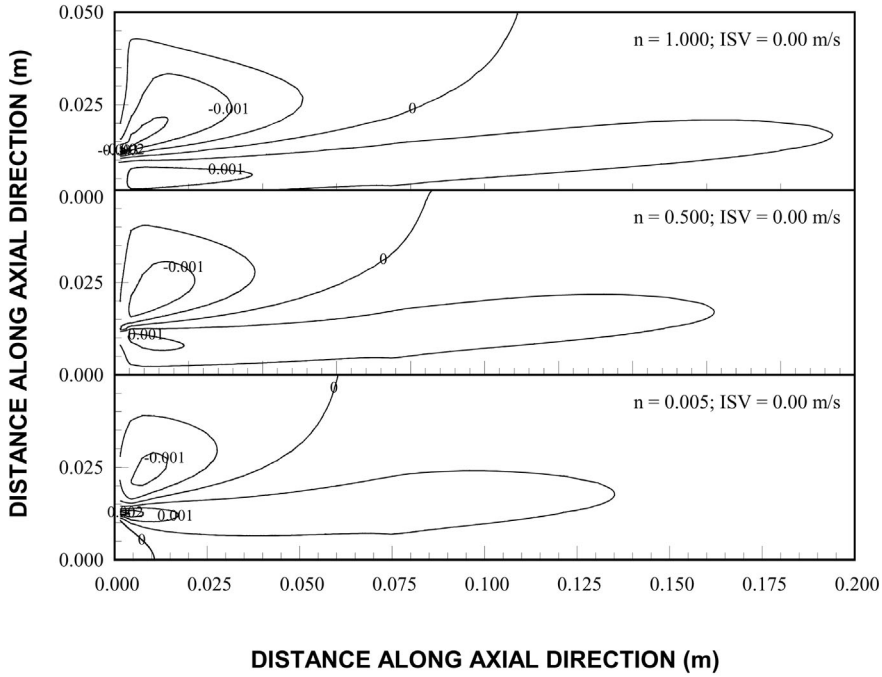

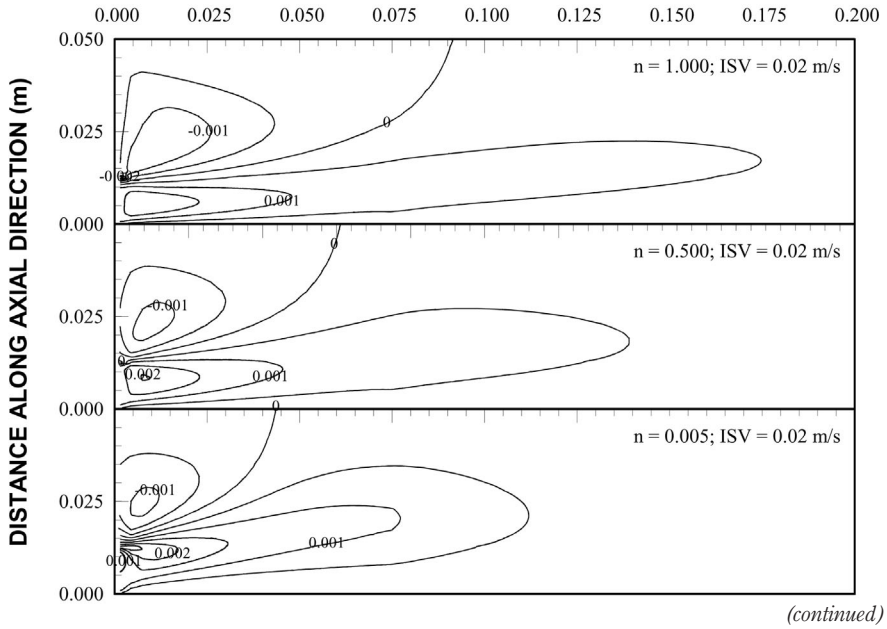

Figure 3.
(a) Radial velocity contours corresponding to different flow configurations. *n* is a velocity profile number and ISV represents the inlet swirl velocity. (b) Axial velocity contours corresponding to different flow configurations. *n* is a velocity profile number and ISV represents the inlet swirl velocity

(continued)

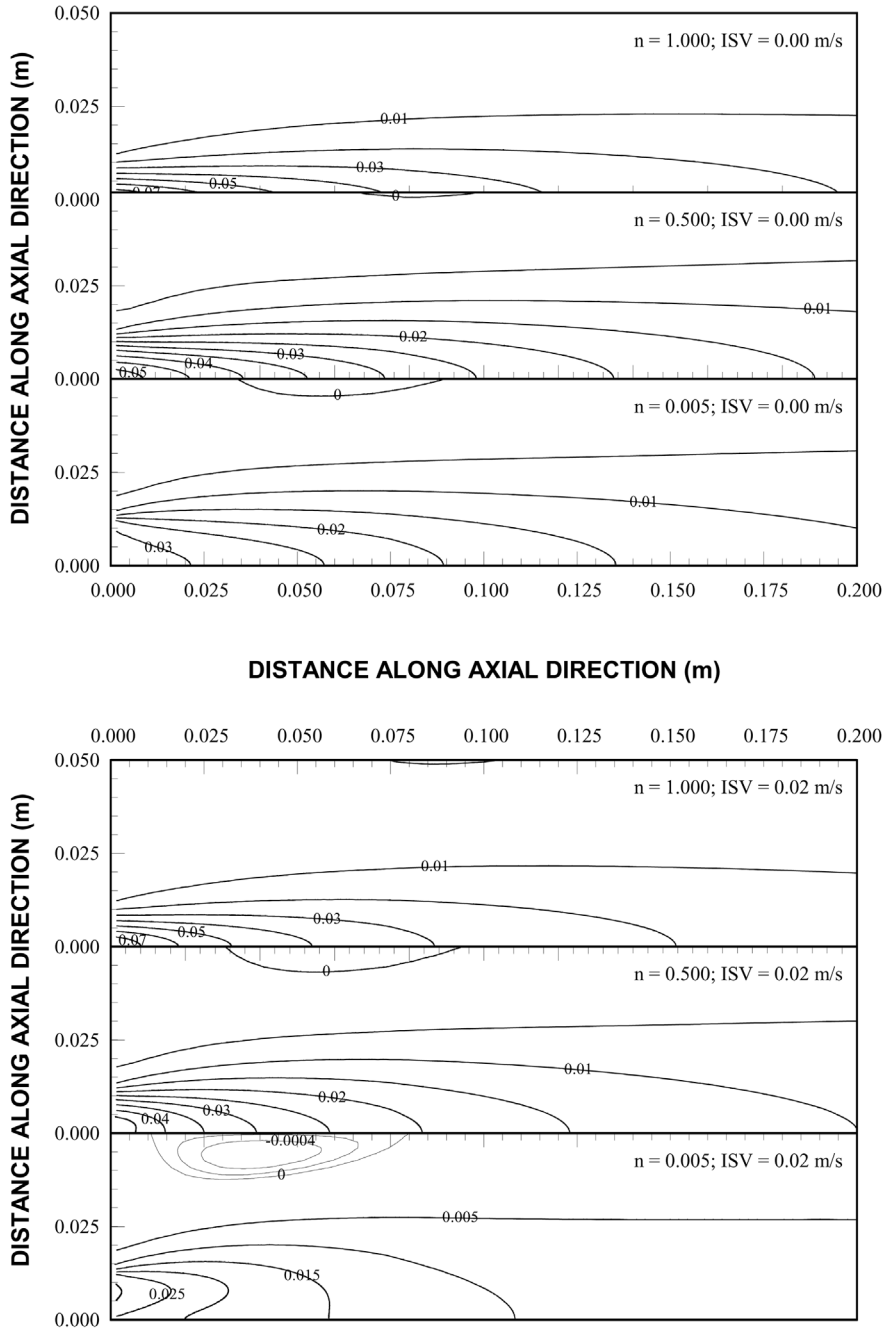
n = 1.000; ISV = 0.00 m/s
n = 0.500; ISV = 0.00 m/s
n = 0.005; ISV = 0.00 m/s
n = 1.000; ISV = 0.02 m/s
n = 0.500; ISV = 0.02 m/s
n = 0.005; ISV = 0.02 m/s
DISTANCE ALONG AXIAL DIRECTION (m)
DISTANCE ALONG AXIAL DIRECTION (m)
0.000
0.025
0.050
0.075
0.100
0.125
0.150
0.175
0.200

Figure 3.

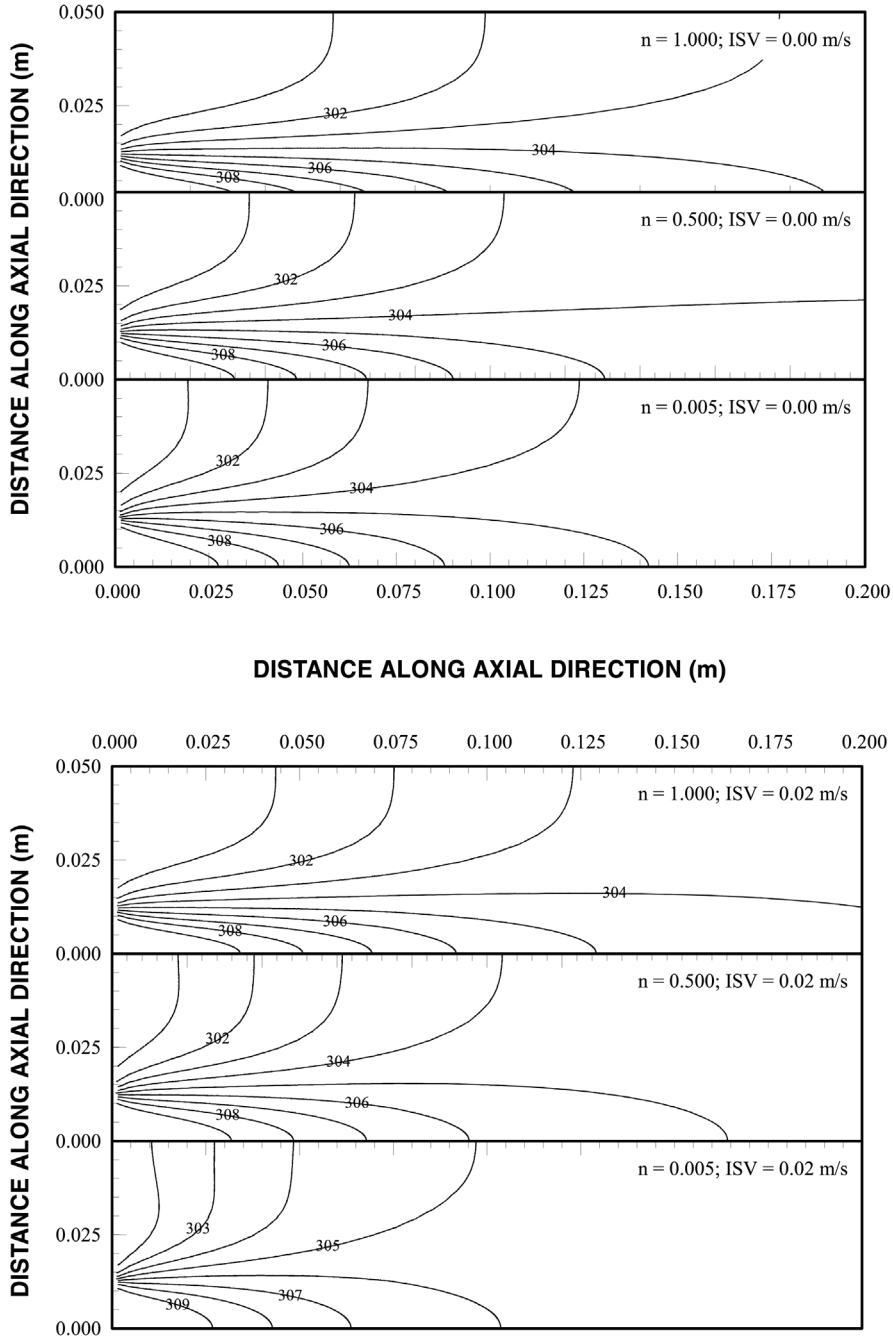

Figure 4.
Temperature contours corresponding to different flow configurations. *n* is a velocity profile number and ISV represents the inlet swirl velocity

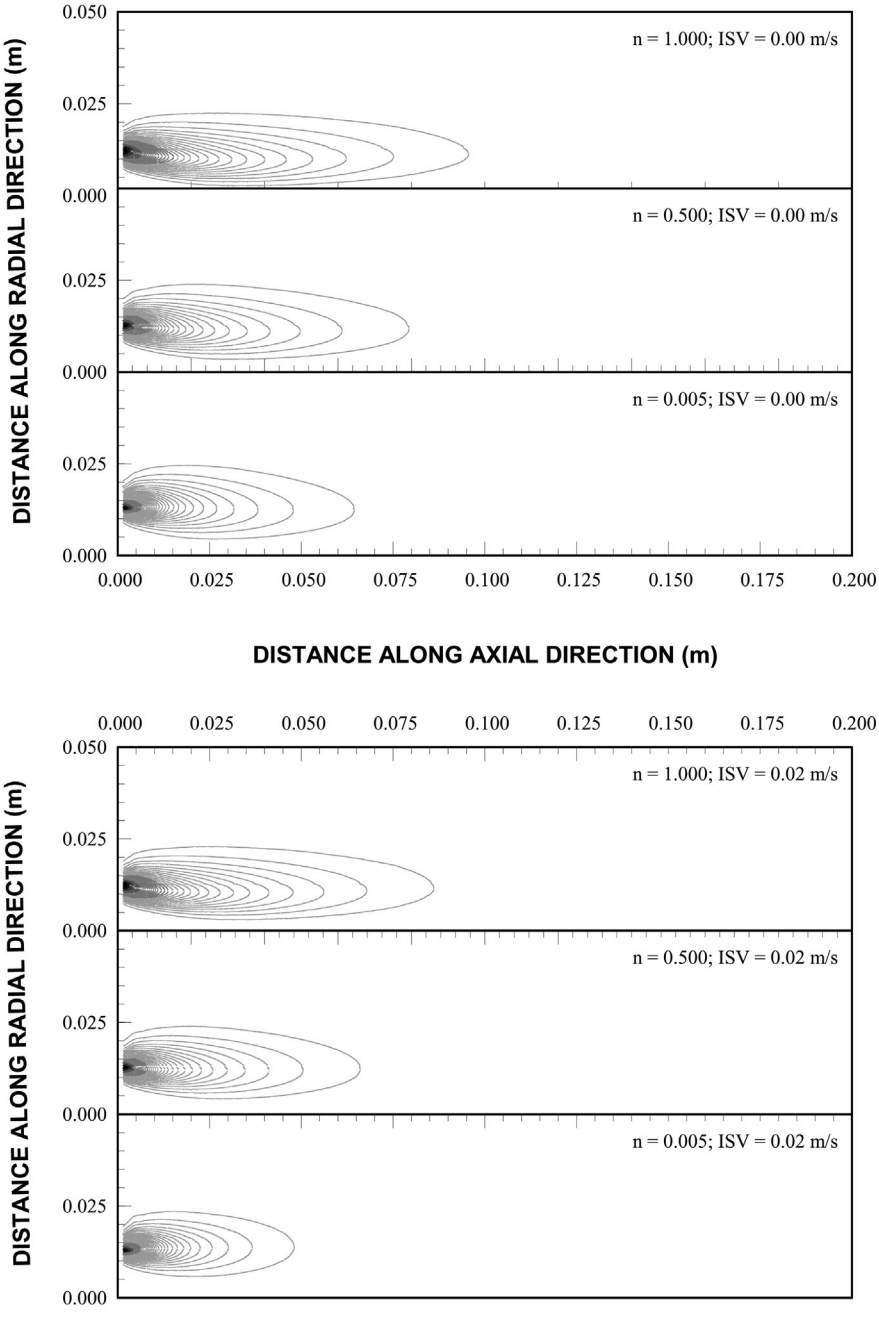

Figure 5.
Entropy generation contours corresponding to different flow configurations n is a velocity profile number and ISV represents the inlet swirl velocity. The profiles are shown in half domain due to axisymmetric situation

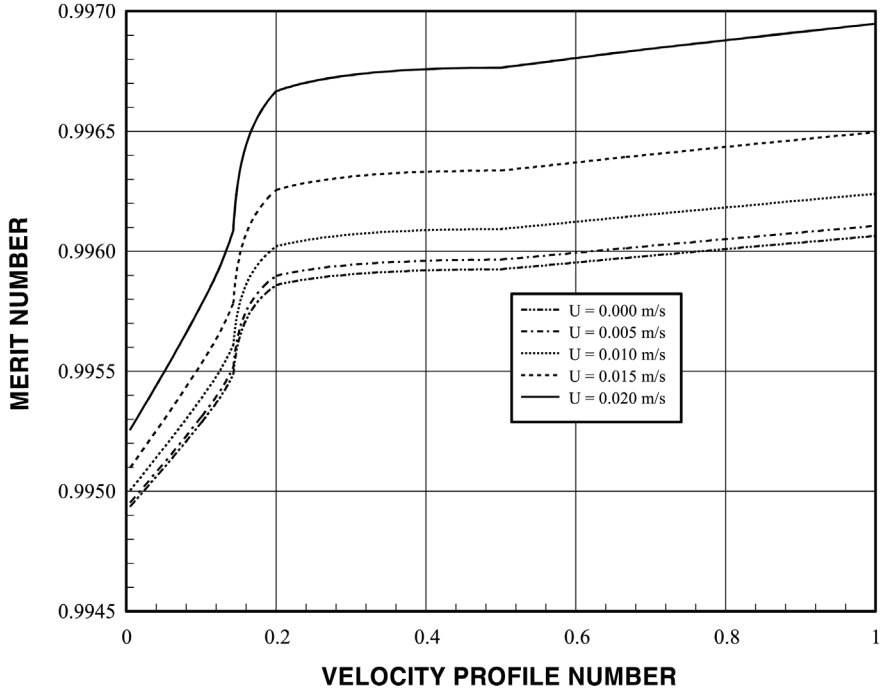

Figure 6.
Variation of normalized total entropy generation with velocity profile number for different swirl velocities

extends further into the downstream. Since the contribution of entropy generation due to heat transfer to the total entropy generation is considerably higher than that corresponding to the fluid friction contribution, large temperature gradient results in high rate of entropy generation in the system. In the case of low velocity profile number (uniform-like velocity profile), jet does not extend considerably in the downstream. Although the temperature gradient across the jet boundary is similar to the triangle-like velocity profile, shortening of the jet length in the axial direction reduces the entropy generation rate. The swirling of the jet results in the jet extension in the radial direction as well as shortening the jet length in the axial direction. This has two-fold effects:

(1) the temperature gradient across the jet reduces after the radial expansion of the jet, and

(2) high temperature gradient does not extend further into the downstream flow.

Consequently, attainment of low temperature gradient and shortening of the jet in the axial direction reduces the entropy generation rate considerably. This is more pronounced at low velocity profile numbers, i.e. uniform-like velocity profile results in less entropy generation. As the velocity profile number reduces, the entropy generation also reduces. This is more pronounced at high

swirl velocity ($u = 0.020\,\mathrm{m/s}$). Consequently, increasing swirl velocity reduces the entropy generation rate, and this signifies when velocity profile number reduces.

Figure 7 shows the variation of Merit number with velocity profile number for different swirl velocities. Merit number represents the maximum heat transfer rate to sum of maximum heat transfer rate and the total irreversibility. In this case, higher the Merit number higher are the maximum heat transfer rates. Since the flow system is not involved with the work production, the second law efficiency analysis for the measure of the irreversibility may not be appropriate. Therefore, the Merit number is presented as consistent with the previous study (Mukherjee *et al.*, 1987). Merit number attains low values at low velocity profile number despite the fact that entropy generation rate is low at low velocity profile numbers. This indicates that uniform like velocity profile results in relatively less heat transfer rates. This is because the relatively shorter jet length in the axial direction as compared to other jet profile numbers, i.e. short jet length reduces the heat transfer surface between the jet and the low temperature flow around the jet. Moreover, as the swirl velocity increases, the Merit number increases. In this case, expansion of the jet at high swirl velocity enhances the heat transfer rates and reduces the irreversibility of the system.

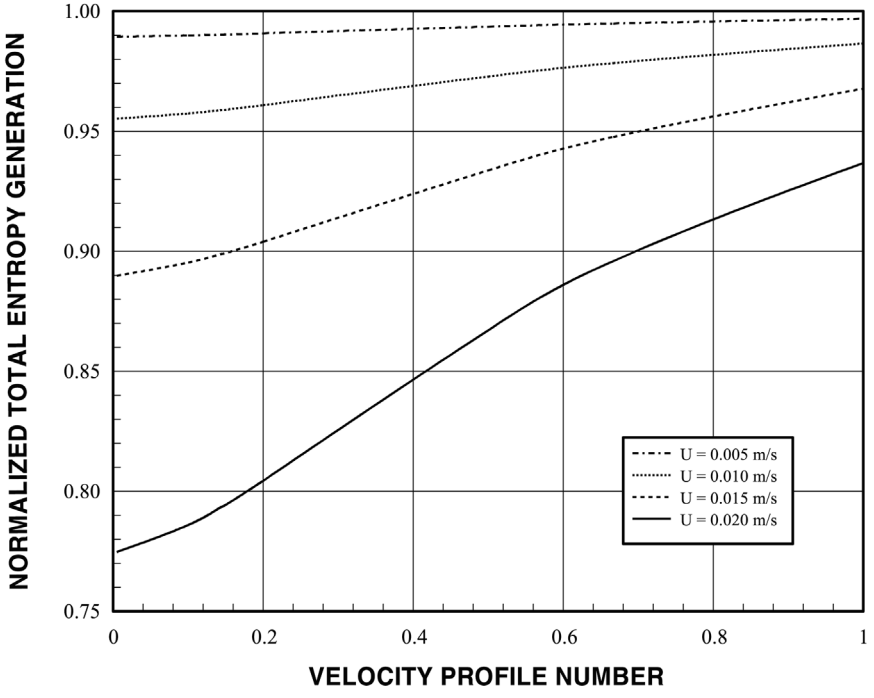

Figure 7.
Variation of merit number with velocity profile number for different swirl velocities

Conclusions

A confined laminar swirling jet with different jet exiting velocity profiles is studied. The flow and temperature fields are simulated using a control volume approach. Entropy generation due to fluid friction and heat transfer are computed. It is found that swirling expands the jet in the radial direction and reduces the jet length in the axial direction. Entropy generation rate reduces as swirl velocity increases. This is more pronounced for uniform-like jet exiting velocity. Merit number attains low value for the uniform like velocity profile despite the low entropy production rate. The specific conclusions derived from the present study are listed as follows:

(1) Uniform-like velocity profile results in a circulation cell next to the jet boundary in the region close to the jet exit. The size of the circulation cell increases as the swirl velocity increases. The effect of swirling on the flow field is more pronounced at low velocity profile number where the jet exiting velocity is uniform-like.

(2) Temperature profiles follow velocity profiles in the jet, i.e. expansion of the jet due to swirling results in expansion of the temperature contours in the jet.

(3) Total entropy generation reduces for the uniform-like jet exiting velocity profile, in this case, the temperature gradient across the jet reduces slightly and the jet length in the axial direction decreases. Alternatively, large temperature gradient and increased jet extension into the downstream flow enhances the total entropy generation rate. This is more pronounced as velocity profile number increases.

(4) Merit number improves for the triangle-like velocity profile. In this case, increased extension of the jet length into the downstream and high temperature gradient across the jet boundary enhance the heat transfer rates despite the high irreversibility generated for this particular case.

References

Abu-Hijleh, B.A.K. (1998), "Entropy generation in laminar convection from an isothermal cylinder in cross flow", *Energy*, Vol. 23 No. 10, pp. 851-7.

Bejan, A. (1982), *Entropy Generation Through Heat and Fluid Flow*, Wiley, New York.

Drost, M.K. and White, M.O. (1991), "Numerical predictions of local entropy generation in an impinging jet", *Journal of Heat Transfer*, Vol. 113, pp. 823-9.

Khorrami, M.R. (1995), "Stability of a compressible axisymmetric swirling jet", *AIAA Journal*, Vol. 33 No. 4, pp. 650-8.

Korovkin, V.N. and Sokovishin, Y.A. (1989), "Variation of heat transfer in laminar wall jets with different initial velocity profiles", *Applied Thermal Sciences*, Vol. 2 No. 1, pp. 30-2.

Li, H. and Tomita, Y. (1994), "Characteristics of swirling flow in a circular pipe", *ASME Journal of Fluids Engineering*, Vol. 116, pp. 370-5.

Maveety, J.G. and Razani, A. (1996), "A two-dimensional numerical investiagion of the optimal removal time and entropy production rate for a sensible thermal storage system", *Energy – The International Journal*, Vol. 21 No. 12, pp. 1265-76.

Mukherjee, P., Biswas, G. and Nag, P.K. (1987), "Second-law analysis of heat transfer in swirling flow through a cylindrical duct", *ASME Journal of Heat Transfer*, Vol. 109, pp. 308-13.

Nikjooy, M. and Mongia, H.C. (1991), "A second-order modeling study of confined swirling flow", *International Journal of Heat and Fluid Flow*, Vol. 12 No. 1, pp. 12-19.

Patankar, S.V. (1980), *Numerical Heat Transfere*, McGraw-Hill, New York.

Ruocco, G. (1997), "Entropy generation in conjugate heat transfer from a discretely heated plate to an impinging confined jet", *International Communications in Heat and Mass Transfer*, Vol. 24 No. 2, pp. 201-10.

Sheen, H.J., Chen, W.J. and Jeng, S.Y. (1996), "Recirculation zones of unconfined and confined annular swirling jets", *AIAA Journal*, Vol. 34, pp. 572-9.